Simplified Approach for Seismic Risk Assessment of Cabinet Facility in Nuclear Power Plants Based on Cumulative Absolute Velocity

Anh-Tuan Cao, Thanh-Tuan Tran, Thi-Hong-Xuyen Nguyen & Dookie Kim

Published online: 18 Dec 2019.

Submit your article to this journal

View related articles

View Crossmark data
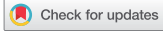
Check for updates

⊗ANS

Simplified Approach for Seismic Risk Assessment of Cabinet Facility in Nuclear Power Plants Based on Cumulative Absolute Velocity

Anh-Tuan Cao,[a] Thanh-Tuan Tran,[a,b] Thi-Hong-Xuyen Nguyen,[a] and Dookie Kim[a]*

[a]*Kunsan National University, Department of Civil and Environmental Engineering, 558 Daehak-ro, Gunsan-si, Jeollabuk-do, Korea*
[b]*Quy Nhon University, Faculty of Technology and Technique, Quy Nhon, Vietnam*

Abstract — *This paper proposes a simplified approach for assessing and predicting the seismic risks for electrical cabinets in nuclear power plants (NPPs). The method is a combination of fragility analysis and cumulative absolute velocity (CAV) analysis. First, the high confidence of low probability of failure points from the fragility curves are defined to determine the CAV_{limit} capacity of the cabinet. Then, the potential damage to the electrical cabinet at different locations in Korea is considered via probabilistic seismic maps. Based on the CAV_{limit} capacity, a seismic risk assessment is conducted to observe the operant condition or predict the potential issues of the electrical cabinet under seismic effects.*

An electrical cabinet is used as a setting for numerical simulation. The finite element model is validated against the experimental results and calibrated by using response surface methodology. Numerical results show that the operant condition of the electrical cabinet can be disturbed by probable earthquakes that have CAV values greater than the CAV_{limit} of 0.27 g·s. This method is one way that NPP operators can follow to obtain cabinet safety regulations.

Keywords — *Seismic risk assessment, cumulative absolute velocity, response surface methodology, fragility analysis, seismicity maps.*

Note — *Some figures may be in color only in the electronic version.*

I. INTRODUCTION

Electric power plays a key role in the socioeconomic development of any country in the world. There are many ways to produce electricity. One of the best options is nuclear power because nuclear energy provides electricity without producing large amounts of carbon emissions and has a low environmental impact on land and natural resources.[1] In the nuclear industry, the electrical cabinet is an indispensable component and contains many electrical devices installed inside it such as distribution panel, switchboard, lighting panel, and other devices for various

purposes. Although the electrical cabinet is just a small part of the nuclear power plant (NPP), it directly affects the operant condition of the NPP when damage occurs. Therefore, the seismic performance of the cabinet should be carefully considered.

Prediction and assessment of seismic risk for NPP components are suggested and even required by many governments. Since the first reactor began commercial operation in 1978, Korea has had no significant nuclear accidents. But, the nuclear disaster in Fukushima, Japan, in March 2011 has created serious concerns for the safety of the NPPs operating in Korea. The Fukushima Daiichi event is the first catastrophe that occurred simultaneously at numerous NPPs at a site.[2]

*E-mail: kim2kie@kunsan.ac.kr

1

A prerequisite of NPP construction is to ensure the safety of the public and the environment from internal and external hazards.[3,4] Safety investigations of NPP components are ordinarily carried out to evaluate the risks to structures in the event of an earthquake. In the nuclear power industry, nuclear facilities are designed to resist ground motion[5–7] (GM). At present, the procedures to assess the performance of components of the cabinet under seismic loading conditions are identified as follows:

1. Create a prototype of the cabinet, and check it by experimental tests.

2. Simulate the numerical model using structural software.

The results from both these steps are compared to accurately predict the behaviors of the structure. The final model can be used to assess many severe circumstances, which helps to surmount any weakness of the shaking table test. Governmental or professional organizations will obtain these data as a part of the safety assessment of NPPs.

Recently, inspections were conducted considering aspects of conditions of specific sites. In Korea, the density of NPPs per site and the population around each plant are quite high. Thus, the concern and urgency of investigating the site risks are significantly higher than in other countries.[8] Boutaraa et al.[9] indicated that seismic risk assessment has been conducted to establish strategies to mitigate the hazard. There is some historical information to estimate the preliminary seismic effects in Korea, including seismic source models, which seismicity experts proposed based on recorded GMs from 2000 (Ref. 10). In the current study, we consider seismicity maps in the Korean peninsula. We developed the KS_MAP software at the Kunsan National University Structural System Laboratory to define the peak ground acceleration (PGA) values for estimating the damage that can occur in structures. The software is available on the Kunsan National University Structural System Laboratory website (http://kim2kie.com/).

This study proposes an applicable method that makes estimating the capacity of the electrical cabinet in the NPP easy. The method is a combination of cumulative absolute velocity (CAV) and fragility analysis. Using information from seismicity maps, investigators define the crucial PGA values and then calculate the corresponding CAV to assess the operant condition of the cabinet based on the capacity value of CAV_{limit}. For the fragility analysis, this research is a continuous part of our previous study for an electrical cabinet in an NPP (Ref. 11). High confidence of low probability of failure (HCLPF) points were used to define the capacities of components.[12–15] The number of earthquake motions should be adequate to obtain reliable statistical meaning response results.[16] Based on the historical earthquake data in Korea, 30 sets of GMs provided by the Korea Water Resources Corporation (K-water) are used for checking the seismic behavior of the cabinet because they can better reflect characteristics of frequency and attenuation in this peninsula.

II. METHODOLOGY

In previous research, the correlation of earthquake energy and structural damage as expressed by an alternative GM parameter is CAV (Ref. 17). A new approach for predicting and assessing the seismic risk for a structure is proposed in this study, where structural damage and earthquake energy are expressed by fragility curves and CAV, respectively. The schematic diagram in Fig. 1 illustrates the process of this methodology. First, the capacity of the structure CAV_{limit} is calculated based on the combination of the CAV analysis and fragility analysis. Second, the potential range of CAV for each location corresponding to the seismicity maps $CAV_{EQ/range}$ is determined. Finally, the operant condition of the structure is assessed via CAV_{limit} and $CAV_{EQ/range}$ values.

II.A. Determining the Capacity of the Structure

II.A.1. Seismic Fragility Curves

II.A.1.a. Determination of Prior Fragility Curve Parameters

Fragility curve is one of the best current practices, and it expresses the probability failure of the structure corresponding to the input motion level of the intensity measure[18–20] (IM). There are many methods that can be
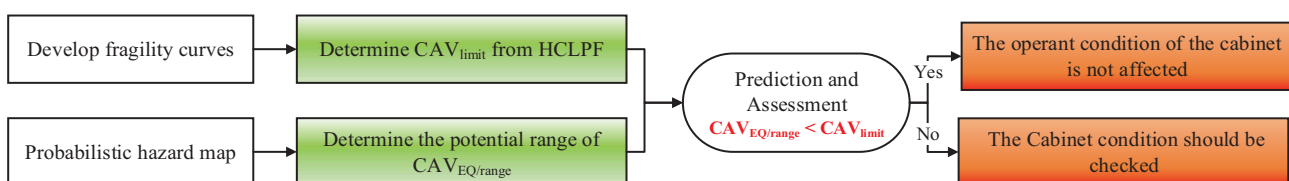
Fig. 1. Risk prediction and assessment processes.

used to develop the fragility curve; one is the classical approach, which is a lognormal method that has been applied in many types of research.[11] Cai et al.[6,7] indicated that the correlation coefficient between $\ln(S_a)$ and $\ln(\text{PGA})$ is a value of approximately 1 and established fragility curves based on the median θ and logarithmic standard deviation β values. In the current study, we apply lognormal approaches including maximum likelihood estimation (MLE) and linear regression (LR) to develop the fragility curves.[11] Furthermore, we consider the acceleration response at the top of the electrical cabinet as the limit state (LS) in the fragility analysis. The shaking table tests that the U.S. Nuclear Regulatory Commission carried out to estimate the probabilistic fragility levels for electrical equipment in NPPs, including switchboard, motor control center, power supply, and panel board, resulted in our selecting the acceleration response as the engineering demand parameter, which we used to conduct the fragility analysis because of reasonable accuracy. The LS is determined when the zero period acceleration reaches 1.8 g.

Maximum likelihood estimation—The MLE method is used, and the fragility curves are established by a particular damage state (DS) given the IM (Ref. 21). The fragility function can be written as follows:

$$P(\text{DS}|\text{IM}) = \Phi\left[\frac{1}{\beta}\ln\left(\frac{\text{IM}}{\theta}\right)\right], \qquad (1)$$

where

P = probability that a GM with IM = x induces the collapse of a structure

$\Phi[.]$ = standard normal cumulative distribution function

θ, β = median and standard deviation of the fragility function, respectively.

Assuming that the IM = x_j for each GM is independent, the likelihood function can be expressed by Eq. (2):

$$Likelihood = \prod_{i=1}^{m} [P(\text{DS}|\text{IM})]^{p_i}[1 - P(\text{DS}|\text{IM})]^{1-p_i}, \qquad (2)$$

where

m = number of IM levels

Π = product over all levels

p = 1 or 0 depending on whether or not the cases exceed the LS.

The fragility function parameters θ and β are obtained by maximizing the likelihood function.

Linear regression—This is a seismic demand model using the power function described in Eq. (3) (Ref. 22):

$$D(\text{IM}) = a \cdot (\text{IM})^b \cdot \epsilon, \qquad (3)$$

where

ϵ = lognormal random variable with a median of 1 and a logarithmic standard deviation $\beta_{D|\text{IM}}$

a, b = model parameters calculated using a LR analysis for the seismic demand model in the transformed logarithmic space in the following form:

$$\ln(D(\text{IM})) = \ln(a) + b\ln(\text{IM}) + \varepsilon, \qquad (4)$$

where $\ln(D(\text{IM}))$ is the expected value for the natural logarithm of DS given IM. The demand model is described as a straight line from a log-log plot of the IM-DM relationship, and dispersion of $\beta_{D|\text{IM}}$ describes the uncertainty in their relationship. The fragility function with the median $\theta_m = \exp[(\ln(\text{DS}) - \ln(a))/b]$ is rewritten as follows:

$$P(\text{DS}|\text{IM}) = \Phi\left[\frac{\ln\left(\frac{\text{IM}}{\theta_m}\right)}{\frac{\beta_{D|\text{IM}}}{b}}\right]. \qquad (5)$$

Parameter $\beta_{D|\text{IM}}$ is obtained as a logarithmic standard deviation of errors, which is explained in Eq. (6):

$$\beta_{D|\text{IM}} = \sqrt{\sum_{i=1}^{N} (e_i)^2/(N-2)}, \qquad (6)$$

where e_i is the residual between the actual value $\ln(D_i)$ and the value predicted by the linear model.

II.A.1.b. Updating the Fragility Curves

In order to update the fragility curves, the Monte Carlo simulation (MCS) approach is proposed.[23] The main steps of the process are described as follows:

Step 1: The prior fragility parameters including median θ and logarithmic standard deviation β are determined.

Step 2: MCS is used to generate a "collect data."

Step 3: The estimated fragility parameters are calculated based on the data in step 2.

Step 4: Repeat steps 2 and 3 many times to estimate the posterior fragility curves.

II.A.2. CAV Analysis

In the NPP field, CAV is a common IM that helps the operators decide whether or not the plant must be shut down after an earthquake event. CAV is determined as the integral of the absolute values of acceleration in the whole time domain, which is expressed mathematically by Eq. (7) (Ref. 24):

$$CAV = \int_0^{t_{max}} |a(t)| dt, \tag{7}$$

where

$$t = \text{time}$$

$$t_{max} = \text{whole duration}$$

$$|a(t)| = \text{absolute acceleration value.}$$

Obviously, CAV increases with time until getting the maximum value at t_{max}. The total effects of an earthquake event will be included and reflected by CAV. Therefore, the Electric Power Research Institute (EPRI) stated that CAV is one of the best GM IMs to express the characteristic of an earthquake. EPRI proposed the CAV value of 0.3 g·s for checking the whole NPP condition, but in the current study we focus on evaluating the performance of just the cabinet. Some versions of CAV were developed by various researchers. One of them is a standardized version called CAV_{STD}, which eliminates the nondamaging components and the contribution of the small-acceleration amplitude of seismic excitation. The formula is explained by Eqs. (8) and (9):

$$CAV_{STD} = \sum_{i=1}^{N} \left(H(PGA_i - \ddot{u}_{min}) \int_{i+1}^{i} |a(t)| dt \right) \tag{8}$$

and

$$H(\delta) = \begin{cases} 0 & \delta < 0 \\ 1 & \delta \geq 0 \end{cases}, \tag{9}$$

where

$$N = \text{number of nonoverlapping acceleration values for 1-s time intervals}$$

$$PGA_i = \text{PGA value in } i\text{'th time step } (g)$$

$$\ddot{u}_{min} = \text{threshold value of acceleration (normally 0.025 } g \text{ is taken) to eliminate small amplitude}$$

$$H(\delta) = \text{Heaviside step function.}$$

Figure 2 illustrates the graphical expression of CAV and CAV_{STD}.

In addition, another version called CAV_5, explained by Kramer and Mitchell, is CAV after applying the threshold value of 5 cm/s (Refs. 2 and 25). Nevertheless, Campbell and Bozorgnia indicated that the elimination of small-amplitude acceleration from CAV, especially values near threshold, induces instability in estimating these IMs (Ref. 17). Therefore, only the original CAV method is used in this paper.

The CAV_{limit} capacity of the electrical cabinet is defined using the CAV method based on the PGA values of the HCLPF point from the fragility curves. The fragility curves of the electrical cabinet reflect the vulnerability of the structure. In 1994, Reed and Kennedy stated that the HCLPF capacity is defined to be the 95% confidence of a 5% probability of exceedance.[26] In addition, in 2018, Sen stated that the 5% probability of structural failure is a common level in all civil engineering structures for checking the safety against earthquakes.[27] Therefore, the PGA value of the HCLPF point is used for scaling the earthquake data set to check the capacity of the electrical cabinet. Obviously, various earthquakes have different CAV values although they have the same PGA. Therefore, to be more conservative, the lowest value of CAV has been chosen as the capacity of the electrical cabinet because of its important role in NPPs.
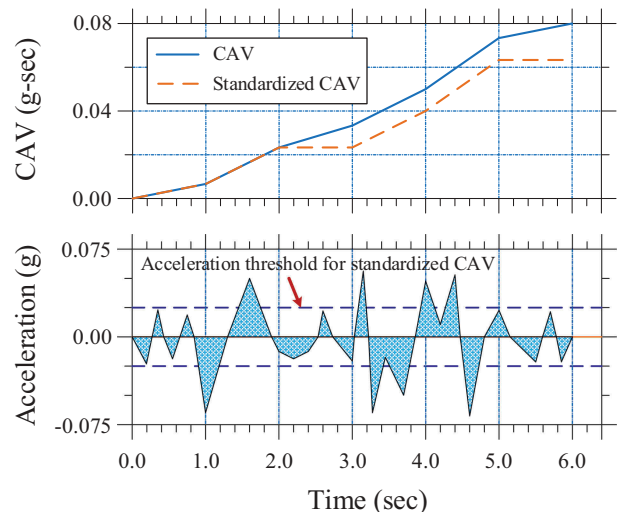
Fig. 2. CAV definition.[17]
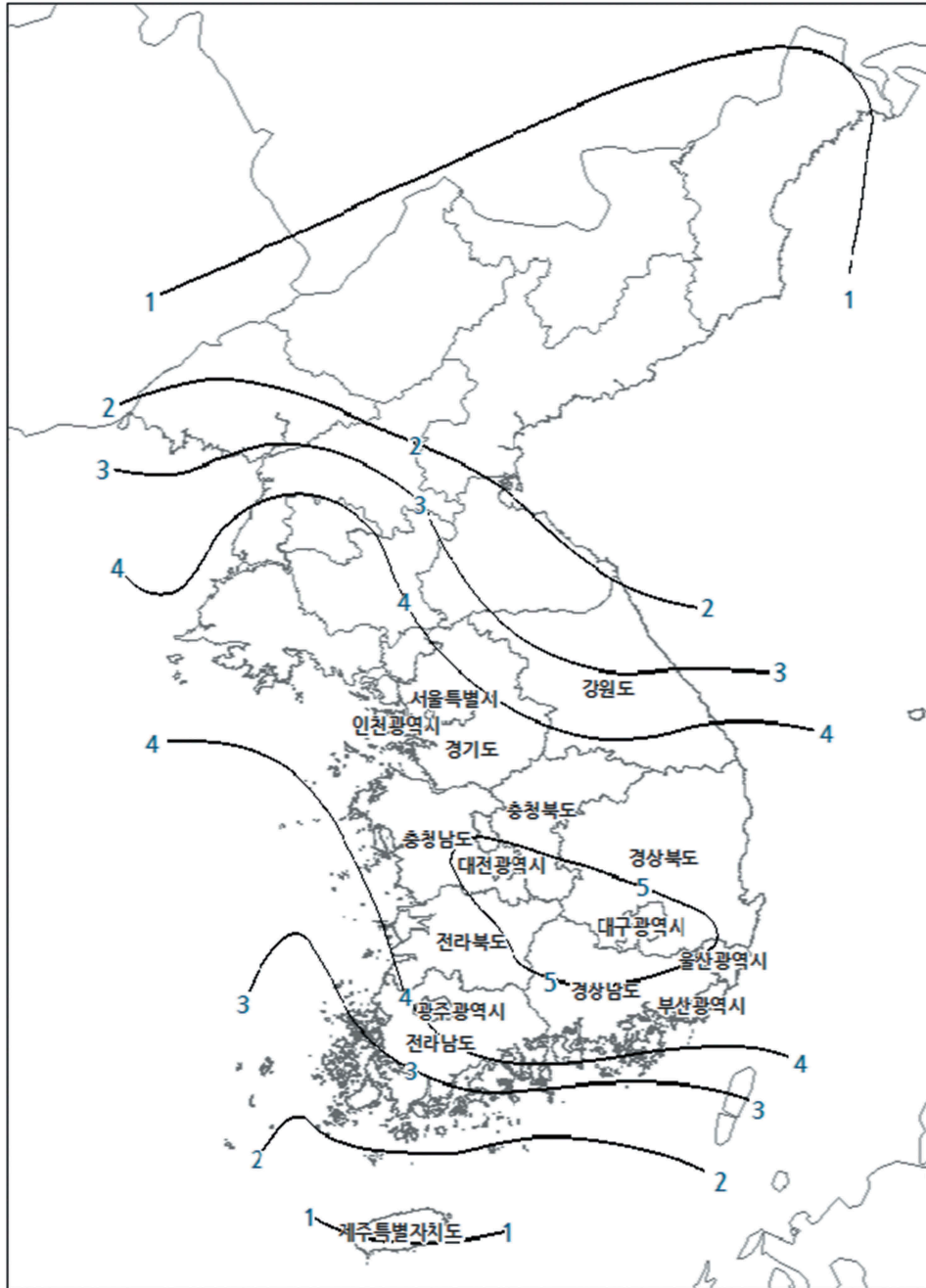
Fig. 3. Seismicity maps in the Korean peninsula (return period is 100 years).

II.B. Calculating the Potential Range of CAV at NPP Locations

II.B.1. Probabilistic Hazard Maps of the Korean Peninsula

The site-specific PGA is pertinent for use in seismic risk assessment because the PGA is a common IM and the practical value, which represents the size of an earthquake. In order to find out the potential PGA at a specific NPP location, seismicity maps are recommended. This study uses seismicity maps of the Korean peninsula that were established based on historical earthquake data.[28] The Korean peninsula has been known as a low and average seismicity area; however, checking and predicting the potential effects of earthquake excitation on a structure are always significant, especially in the case of the nation's infrastructure and NPPs. In order to conduct the seismic risk analysis, four seismicity maps corresponding to different return periods are

TABLE I

Seismic Performance Targets and Design GM Levels

Return Period	Description	Level			
		Perform Function	Immediate Recovery	Long-Term Recovery Life Protection	Collapse
50 100 200 500 1000	Level OP Level IO Level LS Level CP	II-rating I-rating class	II-rating I-rating class	II-rating I-rating class	II-rating I-rating

used to define the PGA for each site; one of them is shown in Fig. 3.

II.B.2. Defining the CAV-PGA Relationship

Development of the relationship between CAV and IM (I_{JMA}) was described by Campbell and Bozorgnia, who considered the instrumental seismic intensity for expressing structural damage.[17] In the current study, we use the same idea but use the conventional IM of PGA from fragility curves. For determining the typical range of CAV at the NPP site, the main procedures should be done as follows:

1. The potential PGA value corresponding to various GM levels at a specific site must be defined based on the seismicity maps.

2. From the design GM levels and earthquake data sets in Korea, the equation expressing the relationship between PGA and CAV can be determined.

In order to define the potential PGA value at any location in Korea, we developed KS_MAP as a part of this study. We used probabilistic hazard maps of the Korean peninsula with the return periods of 100, 200, 500, and 1000 years corresponding to the operational performance (OP), immediate occupancy (IO), life safety (LS), and collapse prevention (CP) levels. Table I expresses the seismic performance level corresponding to different return periods. KS_MAP provides a rapid determination of the PGA at any location with various return periods.[29]

II.C. Seismic Risk Prediction and Assessment

After estimating the CAV_{limit} capacity of the electrical cabinet and the potential range of $CAV_{EQ/range}$ at the NPP sites, these values should be compared to predict the seismic risk of the structure. In addition, based on

CAV_{limit}, the operant condition of the structure can be checked with any earthquake by calculating the CAV of these events. If the CAV value of the certain earthquake is greater than CAV_{limit}, the shutdown decision for the cabinet must be required.

III. APPLICATION FOR CABINET FACILITY IN NPPS

III.A. NPPs in Korea

Korea is well-known over the world to be a prominent country regarding nuclear energy and recently has even turned to exporting its technology to other countries such as Jordan and the United Arab Emirates. Having been an energy importer, Korea has been constructing NPPs as an audacious goal for Korea's development. Korea Hydro & Nuclear Power (KHNP) was established in recognition of the important role of NPPs and the severe consequences if disaster occurs. KHNP's purpose is to continuously improve safety against seismic hazards for all NPPs in Korea.

At present, there are four main plant sites operating in Korea, and different locations will have different potential seismic impacts; therefore, seismic risk should be adequately evaluated. In this study, one prototype of the electrical cabinet is used and checked for four locations. Figure 4 shows all of the NPP sites in Korea, and the corresponding coordinates are listed in Table II.

III.B. Numerical Modeling of the Electrical Cabinet in NPP

III.B.1. Description of the Electrical Cabinet

The NPPs use a wide range of electrical cabinets with various specific combinations of variables such as cabinet

Fig. 4. NPPs in Korea (source: World Nuclear Association).

dimensions, electrical loads, and vent openings.[30] Being indispensable equipment in the NPP, the electrical cabinet has many electrical devices installed inside, which are expressed in Fig. 5a. Thus, the seismic vulnerability of this equipment should be evaluated.[31] Figure 5b shows the prototype of the electrical cabinet provided by the Innose Tech company in Korea to carry out the shaking table test. Figure 5c shows the finite element model of the electrical cabinet, which is simulated using SAP2000.

The cabinet's components including mainframe, subframe, and plate are assigned SS400 steel, which has 200 GPa of modulus of elastic; density ρ and Poisson's ratio v are 7850 kg/m^3 and 0.3, respectively. Besides that, the dimensions of the cabinet are $800 \times 800 \times 2100$ mm, and the whole weight is 287 kg; the weight of each door is 43.6 kg.

TABLE II

The Coordinates of NPPs in Korea

Name	Latitude (deg)	Longitude (deg)
Hanbit	35.409	126.416
Hanul	37.098	129.372
Shin Wolsong	35.713	129.476
Shin Kori	35.324	129.294

For a better understanding of the cabinet's dynamic characteristics, both prototype and numerical models are established. After analysis, the responses from the experimental test are compared to the numerical model for updating, and the optimum model can be used to assess various cases to surmount the weakness of doing experiments. Figure 6 describes the section of the electrical cabinet's components.

III.B.2. Calibration and Verification

Response surface methodology (RSM) is applied in this study to optimize the numerical model. RSM is a collection of statistical and mathematical models that are convenient for modeling, analyzing, and building an empirical model.[32] The process of the RSM technique is shown in Fig. 7.

The responses (output) are obtained from several independent variables (input variables) by using the experiment design. Ordinarily, two equations including linear and polynomial equations are used to express the magnitude of the coefficients, which are explained as follows:

linear equation:

$$b = \beta_0 + \sum_{i=1}^{n} \beta_i a_i + \sum_{i,j=1}^{n} \beta_{ij} a_i a_j + u \qquad (10)$$

and

polynomial equation:

$$b = \beta_0 + \sum_{i=1}^{n} \beta_i a_i + \sum_{i=1}^{n} \beta_i a_i^2 + \sum_{i,j=1}^{n} \beta_{ij} a_i a_j + u, \qquad (11)$$

where

b = estimated response

$\beta_0, \beta_i, \beta_{ij}$ = partial regression coefficients of noise

a_i = coded factor $(i, j = 1, 2, 3 \ldots, n)$

u = offset term.

Equations (10) and (11) can be used with higher order, but in solving engineering issues, second order is suitable. In this paper, the total number of experiments is computed using the central composite design (CCD) method by Eq. (12):

$$S = 2^n + 2n + c_p, \qquad (12)$$

where n is the number of factors and c_p is the number of center points. Therefore, the number of experiments in this research is $S = 2^2 + 2 \times 2 + 1 = 9$. The natural frequencies of the cabinet following the x-direction and

(a) Electrical devices   (b) The prototype of cabinet   (c) Finite element model

Fig. 5. Model of the electrical cabinet.

(a) Main frame   (b) Sub frame 1   (c) Sub frame 2
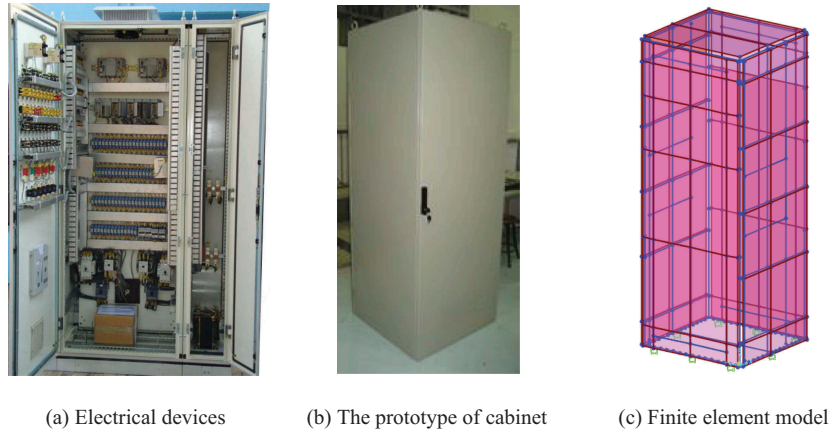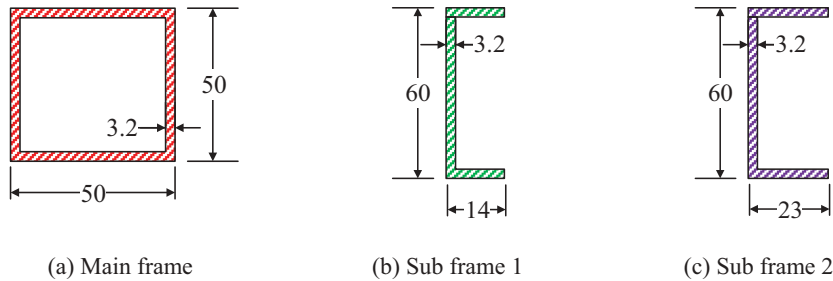
Fig. 6. Electrical cabinet's components.
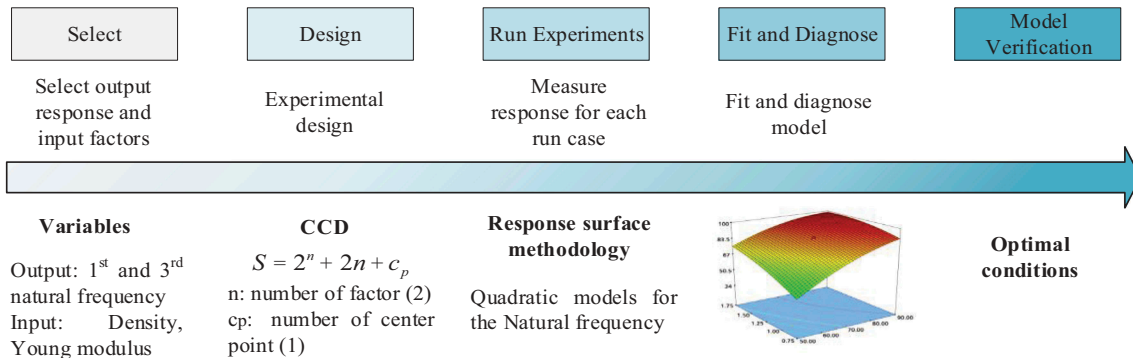
Fig. 7. Optimization process.

y-direction are considered as the target objects corresponding to the first and third modes in the numerical model. Thus, the natural frequency amplitudes of 1st front-back $NF_{1,FB}$ mode and 1st side-side $NF_{1,SS}$ mode have been taken into account as structural responses. The objective function is expressed by Eq. (13):

$$F_k = (NF_k), \qquad (13)$$

where $NF_k, k = 1, 3$ is the natural frequency of the cabinet at mode k. In order to optimize the natural frequency

of the model, Young's modulus (E) and density have been used as design variables of the cabinet, and the set of experiments has been created by the CCD method with the regions of interest of these variables. RSM has been applied to optimize structural performance based on the target value to find out the enriched results. Table III shows the data of various cases including the input parameters and output responses from the numerical model.

From the previous study, Tran et al. stated that the optimal Young's modulus E and density ρ for the material are 224.391 GPa and 7857.5 kg/m³, respectively.[11] To be

TABLE III

The Analysis Cases Using the CCD Method

Run Cases	Point Type	Input Variables		Responses (Hz)	
		E	ρ	$NF_{1,FB}$	$NF_{1,SS}$
1	1	200 000	7850	13.94	14.62
2	1	245 000	7860	15.42	16.18
3	1	245 000	7850	15.43	16.19
4	0	222 500	7855	14.69	15.42
5	−1	222 500	7847.93	14.70	15.43
6	−1	222 500	7862.073	14.69	15.41
7	−1	190 680.19	7855	13.60	14.28
8	−1	254 319.81	7855	15.71	16.49
9	1	200 000	7860	13.93	14.62

more understandable, Table IV compares the responses before and after optimization.

III.C. Results and Discussion

III.C.1. CAV Capacity of the Electrical Cabinet

III.C.1.a. Prior Fragility Parameters

The fragility analysis was conducted in the previous study, which used two methodologies (MLE and LR) and two cases of boundary conditions (restrained and anchored model).[11] The acceleration response at the top of the cabinet is considered as a damaged state for risk assessment. Table V lists the prior values of the median and standard deviation after the fragility analysis was carried out.

III.C.1.b. Posterior Fragility Curves

The posterior distributions are obtained based on the prior parameters, which are shown in Table V. The MCS is used to generate 10 000 samples from the prior distributions. The posterior distributions and fragility curves are displayed in Figs. 8 and 9 for the restrained model and anchored model, respectively. Table VI lists the posterior fragility parameters of the cabinet after updating.

There are many ways to estimate the capacity of a particular structure. In this study, the HCLPF points are defined from fragility curves, and the lowest value of HCLPF has been selected to calculate the conservative and reliable CAV limitation. In the seismic probabilistic risk assessment, the HCLPF capacity is determined to be 95% confidence of 5% probability of exceedance.[33] A 5% probability of failure is an ordinary level in the civil engineering structure field to check the safety against earthquakes.[27] From Figs. 8 and 9, the lowest PGA value of the HCLPF point is 0.158 g corresponding to the anchored model using the MLE method.

In order to calculate the limitation of CAV, all the earthquakes in the data set are scaled into the smallest value of the HCLPF point, which is shown in Fig. 9d with $PGA_{HCLPF} = 0.158g$. Hardy et al.[34] concluded that the CAV values are defined for each free-field component and selected conservatively. The lowest CAV value from the data set of earthquakes is selected as the limitation.

The CAV value of earthquake 1AD in the east-west (EW) direction is displayed in Fig. 10. The CAV calculations

TABLE IV

The Comparison of Structural Responses

	Responses (Hz)		Error (%)	
	$NF_{1,FB}$	$NF_{1,SS}$	$NF_{1,FB}$	$NF_{1,SS}$
Before optimization	14.36	14.64	0.03	0.12
After optimization	14.75	15.5	0.00	0.07

⊗ANS

TABLE V

Prior Fragility Parameters of Cabinet

Approach	Restrained Model		Anchored Model	
	θ^{prior}	β^{prior}	θ^{prior}	β^{prior}
MLE	1.860	0.550	1.180	0.610
LR	1.540	0.670	1.290	0.580

for the rest of the earthquakes are carried out the same way, and their values corresponding to two horizontal components of each earthquake are listed in Table VII.

From Table VII, the minimum CAV values obtained are 0.32 and 0.27 g·s for the north-south (NS) direction and EW direction, respectively. Thus, it can be said that the capacity value of CAV_{limit} for the cabinet is 0.27 g·s.

The CAV check for a potential earthquake is surpassed if any value of the two horizontal components from the free-field excitation is greater than 0.27 g·s. This is mentioned in the research by Campbell and Bozorgnia; if GM CAV exceeds the CAV_{limit} value, the operating basis earthquake is surpassed, and the operant condition of the structure should be checked.[17]
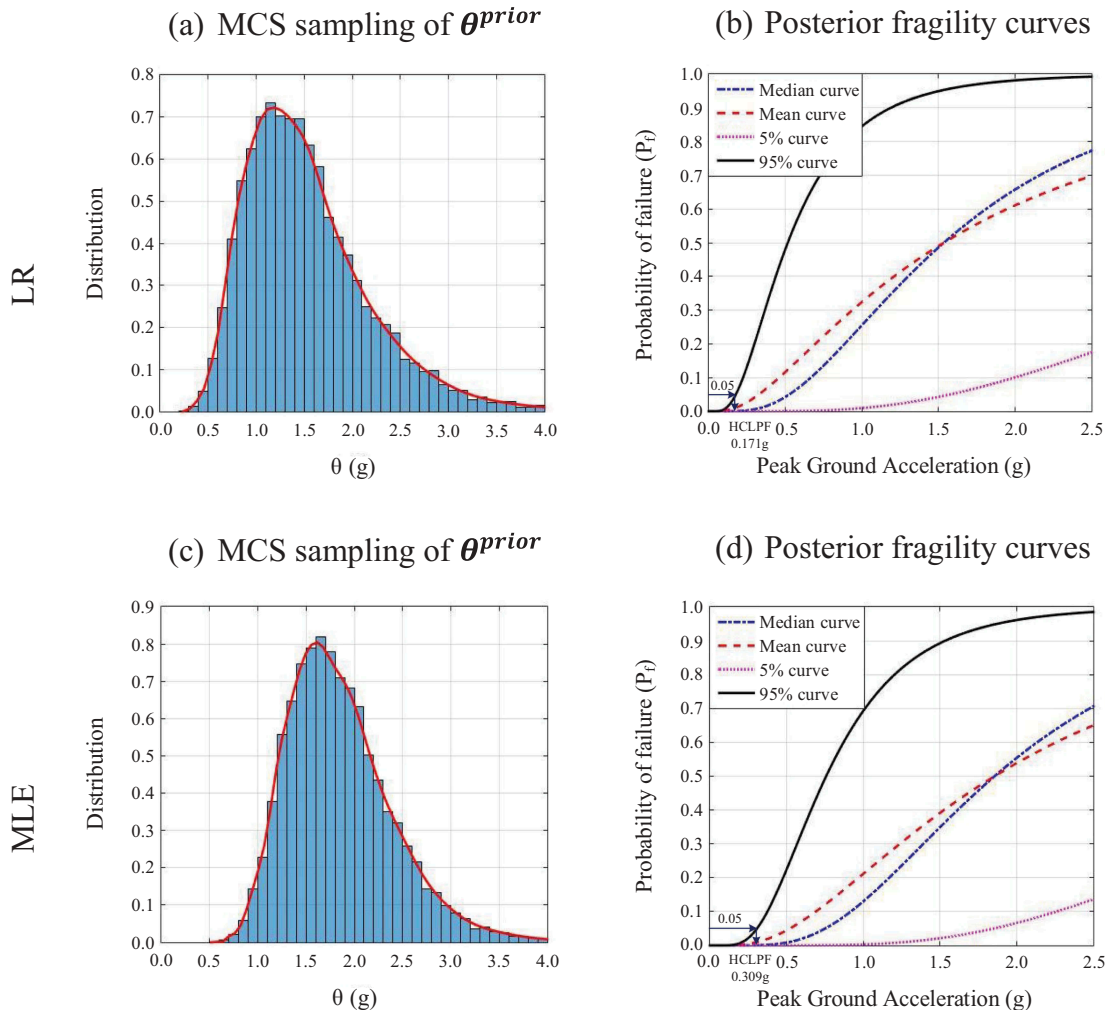
Fig. 8. Fragility curves of the restrained model.

TABLE VI

Posterior Fragility Parameters of Cabinet

Approach	Restrained Model		Anchored Model	
	$\theta^{posterior}$	$\beta^{posterior}$	$\theta^{posterior}$	$\beta^{posterior}$
MLE	1.867	0.543	1.180	0.602
LR	1.541	0.664	1.290	0.574

III.C.2. Relationship of CAV and PGA for NPP Sites

The main purpose of this research is to check the operant condition of the electrical cabinet under potential seismic circumstances, which is based on the potential PGA at the specific location of the NPP site. As noted earlier, as part of this study, we developed the KS_MAP software to define the PGA value at any location in Korea. Probabilistic hazard maps in the Korean peninsula and the Google Map function are used to define the coordinates of the construction site and the corresponding PGA value. KS_MAP provides a rapid determination of the crucial PGA value at any location with various return periods. In order to estimate the potential risk at the NPP site, historical earthquakes in Korea are scaled, and CAV analysis for both horizontal components is

(a) MCS sampling of θ^{prior}

(b) Posterior fragility curves

(c) MCS sampling of θ^{prior}

(d) Posterior fragility curves
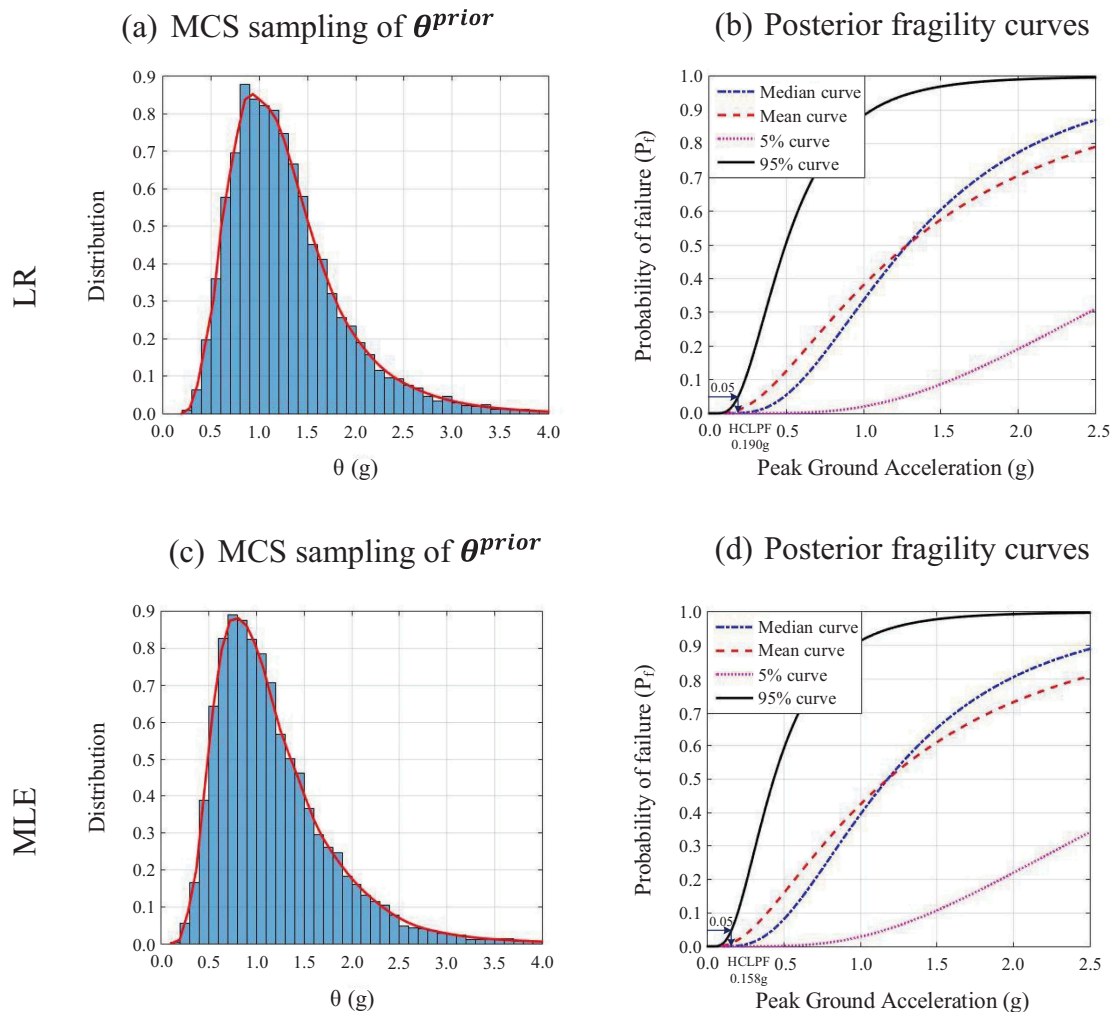
Fig. 9. Fragility curves of the anchored model.

TABLE VII

CAV Values Corresponding to Historical Earthquakes in Korea

Earthquake	CAV-EW ($g \cdot s$)	CAV-NS ($g \cdot s$)
1AD	0.57	0.75
2BA	0.85	0.84
4BJ	1.12	0.70
5BR	1.04	0.96
6BS	0.80	0.66
7CG	0.39	0.54
9CJ	0.56	0.59
10DA	0.82	0.72
11DB	0.43	0.40
12DG	0.87	0.82
13DS	0.27	0.33
14EP	0.70	0.75
15GC	1.04	1.07
16GD	0.38	0.58
17GM	0.87	0.63
18GN	1.72	1.54
19GP	0.31	0.37
20GW	0.60	0.88
21HC	0.74	0.32
22HN	0.71	0.73
23HS	0.51	0.74
24IH	0.60	0.72
26MR	0.83	0.70
27ND	1.08	1.02
28NG	0.69	0.61
29PH	0.70	1.04
30PN	0.75	0.95
31RD	0.58	0.69
35YD	0.74	0.56
36YO	0.93	0.69

conducted. The average CAV value in each component is calculated based on the scaled data, and the greater one is chosen as the typical CAV value. Table VIII summarizes CAV corresponding to PGA values of different levels.

The relationship between PGA and CAV was obtained performing a LR analysis.[35] Hence, the formula generated from the results of this research is linear, and it can be written by the following mathematical term:

$$CAV_{EG/range} = 4.6099 PGA + 0.001 . \qquad (14)$$

From Eq. (14), the potential CAV value can be calculated using the corresponding PGA of any structural performance level. Seismic risk at the NPP site in Korea can be predicted and is expressed in Fig. 11.

Based on the capacity of the electrical cabinet, the operant condition can be evaluated by comparing it with certain or potential earthquakes, as shown in Fig. 11. The main observations are as follows:

1. In general, the electrical cabinet will not be affected at the OP level.

2. For the IO level, the cabinet is still stable at the Hanul and Hanbit sites, but it will be affected at the rest of the sites.

3. Potential damage to the electrical cabinet can happen at the locations of all NPPs in Korea. For the LS and CP levels, the operant condition of the electrical cabinet can be disturbed by probable earthquakes, which can have CAV values greater than $CAV_{limit} = 0.27$ $g \cdot s$.

Although the electrical cabinet is a small part of the NPP, it relates directly to the activities of the plant.

TABLE VIII

Definition of CAV Values of NPPs with Different Levels

Return Period	Level	Hanbit		Hanul		Shin Wolsong		Shin Kori	
		PGA (% g)	CAV (g·s)	PGA (% g)	CAV (g·s)	PGA (% g)	CAV (g·s)	PGA (% g)	CAV (g·s)
100	OP	3.76	0.174	4.24	0.196	4.56	0.211	4.58	0.212
200	IO	4.9	0.227	5.61	0.260	7.0	0.324	6.28	0.291
500	LS	7.3	0.338	8.6	0.397	10.27	0.474	9.13	0.422
1000	CP	10.39	0.480	11.6	0.536	13.26	0.612	11.89	0.549

(a) East-West direction (PGA = 0.158g)   (b) CAV = 0.57 g-sec
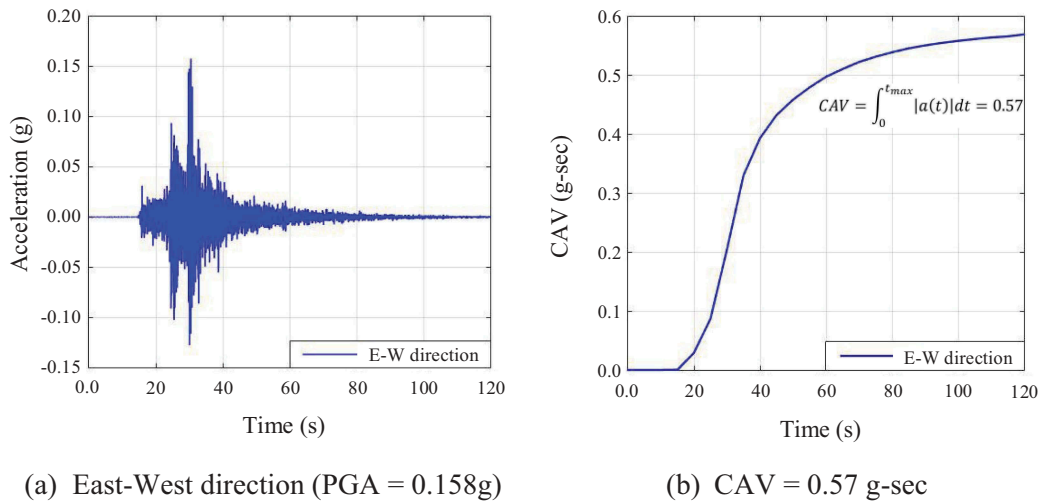
Fig. 10. CAV calculation for earthquake 1AD.
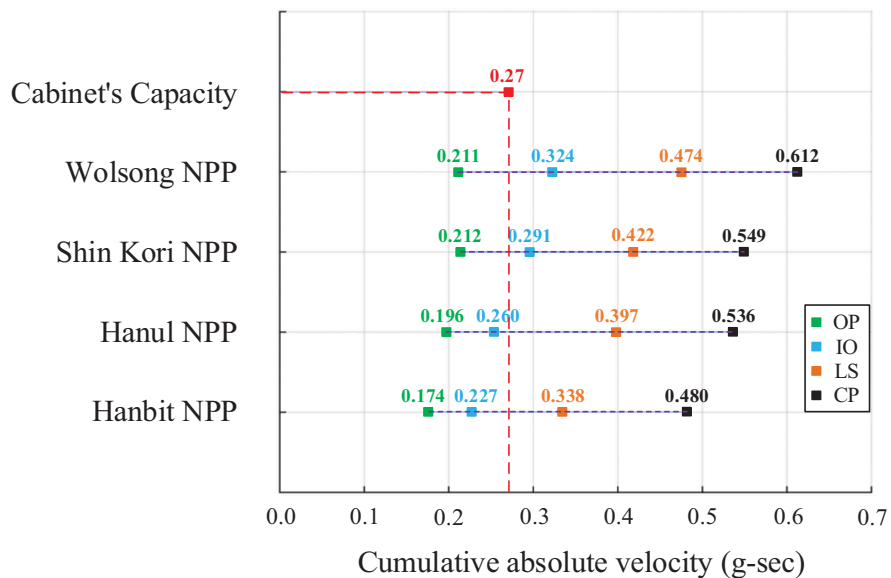
Fig. 11. CAV comparison between the cabinet's capacity and potential earthquakes.

Therefore, seismic risk assessment and prediction are very important to prevent severe consequences.

IV. CONCLUSIONS

This study presents a simplified approach for seismic risk assessment and prediction of the electrical cabinets in NPPs. The method is a combination of CAV and fragility analysis. The proposed approach is adapted for NPP cabinets and corresponds to GM data in Korea. The results indicate that NPP operational inspection can be evaluated with available information such as location (latitude and longitude), data of an earthquake event, etc. In addition, the specific locations in seismicity maps are also taken into account for various NPPs. Within a short time, the method is feasible to estimate the regional distribution of potential CAV.

To make the method practical, the KS_MAP software was developed. Nevertheless, all of the input information needs to be sufficient and reliable including cabinet specifications, responses recorded from the shaking table test, etc. After an earthquake event, free-field motion data would have to be quickly available to determine the operation condition of the structure and if the inspection is required. In reality, the assessment and prediction methods presented in this research are effective because of their time-saving and cost-effectiveness aspects. The developed approach gives early warning action or prevents further failures of the structural components. Using the same process, NPP operators or governmental organizations can flexibly apply different techniques in each step to advance reliability and accuracy.

Acknowledgments

References

1. C. MEDEL-VERA and T. JI, "Seismic Probabilistic Risk Analysis Based on Stochastic Simulation of Accelerograms for Nuclear Power Plants in the UK," *Prog. Nucl. Energy*, **91**, 373 (2016); https://doi.org/10.1016/j.pnucene.2016.06.005.

2. J. E. YANG, "Multi-Unit Risk Assessment of Nuclear Power Plants: Current Status and Issues," *Nucl. Eng. Technol.*, **50**, 1199 (2018); https://doi.org/10.1016/j.net.2018.09.010.

3. J. BOMMER, M. PAPASPILIOU, and W. PRICE, "Earthquake Response Spectra for Seismic Design of Nuclear Power Plants in the UK," *Nucl. Eng. Des.*, **241**, 968 (2011); https://doi.org/10.1016/j.nucengdes.2011.01.029.

4. P. FARSHADMANESH et al., "SHAKE-RoverD Framework for Nuclear Power Plants: A Streamlined Approach for Seismic Risk Assessment," *Nucl. Technol.*, **205**, 442 (2019); https://doi.org/10.1080/00295450.2018.1494439.

5. T. D. VU, D. KIM, and S. G. CHO, "Updating of Analytical Model to Consider Aging Effects of Lead-Rubber Bearings for the Seismic Design of Base-Isolated Nuclear Power Plants," *Nucl. Technol.*, **182**, 75 (2013); https://doi.org/10.13182/NT13-A15828.

6. Z. CAI et al., "Determining Seismic Fragility of Structures and Components in Nuclear Power Plants Using Multiple Ground Motion Parameters—Part I: Methodology," *Nucl. Eng. Des.*, **335**, 195 (2018); https://doi.org/10.1016/j.nucengdes.2018.05.013.

7. Z. CAI et al., "Determining Seismic Fragility of Structures and Components in Nuclear Power Plants Using Multiple Ground Motion Parameters—Part II: Application," *Nucl. Eng. Des.*, **335**, 186 (2018); https://doi.org/10.1016/j.nucengdes.2018.05.016.

8. C. SEONG et al., "Analysis of the Technical Status of Multiunit Risk Assessment in Nuclear Power Plants," *Nucl. Eng. Technol.*, **50**, 319 (2018); https://doi.org/10.1016/j.net.2017.12.015.

9. Z. BOUTARAA et al., "Buildings Vulnerability Assessment and Damage Seismic Scenarios at Urban Scale: Application to Chlef City (Algeria)," *KSCE J. Civil Eng.*, **22**, *10*, 3948 (2018); https://doi.org/10.1007/s12205-018-0961-2.

10. S. KWAG and D. HAHM, "Development of an Earthquake-Induced Landslide Risk Assessment Approach for Nuclear Power Plants," *Nucl. Eng. Technol.*, **50**, 1372 (2018); https://doi.org/10.1016/j.net.2018.07.016.

11. T. T. TRAN et al., "Fragility Assessment for Electric Cabinet in Nuclear Power Plant Using Response Surface Methodology," *Nucl. Eng. Technol.*, **51**, 894 (2019); https://doi.org/10.1016/j.net.2018.12.025.

12. Y. N. HUANG, A. S. WHITTAKER, and N. LUCO, "A Probabilistic Seismic Risk Assessment Procedure for Nuclear Power Plants: (I) Methodology," *Nucl. Eng. Des.*, **241**, 3996 (2011); https://doi.org/10.1016/j.nucengdes.2011.06.051.

13. Y. N. HUANG, A. S. WHITTAKER, and N. LUCO, "A Probabilistic Seismic Risk Assessment Procedure for Nuclear Power Plants: (II) Application," *Nucl. Eng. Des.*, **241**, 3985 (2011); https://doi.org/10.1016/j.nucengdes.2011.06.050.

14. C. MEDEL-VERA and T. JI, "Seismic Probabilistic Risk Assessment of Nuclear Power Plants in the UK: An Alternative Procedure," *Proc. 23rd Conf. Structural*

Mechanics in Reactor Technology, Manchester, United Kingdom, August 10–14, 2015.

15. C. MEDEL-VERA and T. JI, "Seismic Risk Control of Nuclear Power Plants Using Seismic Protection Systems in Stable Continental Regions: The UK Case," *Nucl. Eng. Des.*, **307**, 377 (2016); https://doi.org/10.1016/j.nucengdes.2016.07.031.

16. S. G. GAVABAR and M. ALEMBAGHERI, "Structural Demand Hazard Analysis of Jointed Gravity Dam in View of Earthquake Uncertainty," *KSCE J. Civil Eng.*, **22**, *10*, 3972 (2018); https://doi.org/10.1007/s12205-018-1009-3.

17. K. W. CAMPBELL and Y. BOZORGNIA, "Analysis of Cumulative Absolute Velocity (CAV) and JMA Instrumental Seismic Intensity (IJMA) Using the PEER-NGA Strong Motion Database," University of California, Berkeley, Pacific Earthquake Engineering Center (2010).

18. Y. H. SHEN, Y. N. HUANG, and C. C. YU, "Seismic Probabilistic Risk Assessment of Nuclear Power Plants Using Response-Based Fragility Curves," *Proc. ASME 2014 Pressure Vessels and Piping Conf. (PVP2014)*, Anaheim, California, July 20–24, 2014.

19. Y. N. HUANG and A. S. WHITTAKER, "Seismic Probabilistic Risk Assessment for Nuclear Power Plants," *Infrastructure Systems for Nuclear Energy*, p. 35, John Wiley & Sons (2014); https://doi.org/10.1002/9781118536254.ch3.

20. J. WANG and M. LIN, "Seismic Probabilistic Risk Analysis and Application in a Nuclear Power Plant," *Nucl. Technol.*, **203**, 221 (2018); https://doi.org/10.1080/00295450.2018.1448671.

21. T. K. MANDAL, S. GHOSH, and N. N. PUJARI, "Seismic Fragility Analysis of a Typical Indian PHWR Containment: Comparison of Fragility Models," *Struct. Saf.*, **58**, 11 (2016); https://doi.org/10.1016/j.strusafe.2015.08.003.

22. C. MAI, K. KONAKLI, and B. SUDRET, "Seismic Fragility Curves for Structures Using Non-Parametric Representations," *Front. Struct. Civil Eng.*, **11**, 169 (2017); https://doi.org/10.1007/s11709-017-0385-y.

23. J. W. BAKER, "Efficient Analytical Fragility Function Fitting Using Dynamic Structural Analysis," *Earthquake Spectra.*, **31**, *1*, 579 (2015); https://doi.org/10.1193/021113EQS025M.

24. K. W. CAMPBELL and Y. BOZORGNIA, "Prediction Equations for the Standardized Version of Cumulative Absolute Velocity as Adapted for Use in the Shutdown of US Nuclear Power Plants," *Nucl. Eng. Des.*, **241**, 7, 2558 (2011); https://doi.org/10.1016/j.nucengdes.2011.04.020.

25. S. L. KRAMER and R. A. MITCHELL, "Ground Motion Intensity Measures for Liquefaction Hazard Evaluation," *Earthquake Spectra*, **22**, *2*, 413 (2006); https://doi.org/10.1193/1.2194970.

26. T. T. TRAN and D. KIM, "Uncertainty Quantification for Nonlinear Seismic Analysis of Cabinet Facility in Nuclear Power Plants," *Nucl. Eng. Des.*, **355**, 110309 (2019); https://doi.org/10.1016/j.nucengdes.2019.110309.

27. U. SEN, "Risk Assessment of Concrete Gravity Dams Under Earthquake Loads," Master's Thesis, Louisiana State University and Agricultural and Mechanical College (2018).

28. H. S. LEE, "PBEE in a Moderate-Seismicity Region: South Korea," *Proc. 2017 World Congress Advances in Structural Engineering and Mechanics (ASEM17)*, Ilsan (Seoul), Korea, August 28–September 1, 2017.

29. T. T. TRAN and D. KIM, "Korea Seismicity Map," Kunsan National University Structural System Laboratory website; kim2kie.com (2017) (current as of July 19, 2019).

30. E. AVIDOR et al., "Hazard Assessment of Fire in Electrical Cabinets," *Nucl. Technol.*, **144**, *3*, 337 (2003); https://doi.org/10.13182/NT03-A3449.

31. J. W. REED and R. P. KENNEDY, "Methodology for Developing Seismic Fragilities," EPRI-TR-103959, Electric Power Research Institute (1994).

32. A. I. KHURI and S. MUKHOPADHYAY, "Response Surface Methodology," *WIREs Comput. Stat.*, **2**, *2*, 128 (2010); https://doi.org/10.1002/wics.73.

33. P. Y. YAWSON and D. LOMBARDI, "Probabilistic Seismic Risk Assessment of Nuclear Reactor in a Hypothetical UK Site," *Soil Dyn. Earthquake Eng.*, **113**, 278 (2018); https://doi.org/10.1016/j.soildyn.2018.06.007.

34. G. HARDY et al., "Program on Technology Innovation: Use of Cumulative Absolute Velocity (CAV) in Determining Effects of Small Magnitude Earthquakes on Seismic Hazard Analyses," Product ID 1014099, Electric Power Research Institute (Aug. 2006).

35. L. BAI, "Correlation of the Emergency Handling Peak Ground Acceleration (PGA) for High-Speed Railway and Strong-Motion Indices Using K-net Data," *Proc. 2nd Int. Conf. Civil, Transportation and Environmental Engineering (ICCTE 2017), Advances in Engineering Research*, Vol. 135 (July 2017); https://doi.org/10.2991/iccte-17.2017.12.